

# ICSV14

Cairns • Australia  
9-12 July, 2007



## SIMULATION OF A COMBINED SWITCHED AND INDUCTIVE SHUNT CONTROL ACTING ON A 2D STRUCTURE

Salvatore Ameduri<sup>1</sup>, Monica Ciminello<sup>2</sup> and Antonio Concilio<sup>1</sup>

<sup>1</sup>Laboratory of Smart Structures, The Italian Aerospace Research Centre C.I.R.A. scpa  
Capua, Via Maiorise, Italy

<sup>2</sup>Department of Aeronautical Engineering, "Federico II" University  
Naples, Via Claudio, Italy  
[s.ameduri@cira.it](mailto:s.ameduri@cira.it)

### Abstract

Several control techniques have been developed to improve the reduction of sensitivity of structural elements dynamic response to both parameter variations and disturbances attenuations within the control system bandwidth.

The research activity has shown how passive and active control strategies may be complementary for facing many of the structural dynamic problems. As a matter of fact, while the passive ones demonstrate efficiency for the highest frequencies band, the active systems demonstrate efficiency in a wider broad band domain, despite of the large required power supply and the high cost hardware.

Semi-active controls assure advantages of both passive and active control techniques. In detail, the absence of an external power supply, the reduced vulnerability to power failure, the self-powered architecture, make the semi-active controls simple to be managed and cheaper.

The possibility of jointly implementing both a switched and an inductive shunt architecture may guarantee a more efficient multi mode control. As a matter of fact, it is possible to simultaneously control a low and a high frequency mode through a switch and an inductive architecture. To achieve this result, the RLC parameters of the switch circuit (synchronised on the lower mode) have to be chosen so that its normal frequency is coincident with the higher structural mode to be controlled.

### 1. INTRODUCTION

Numerical and experimental investigations have proved the ability of piezoceramics in passive shunt configuration to control structural vibrations. Different type of shunt circuits have been taken into account but the inductive one is the most widely adopted [1], [2]. By absorbing mechanical vibrations if suitably tuned on specific structural mode, the inductive circuit behaves like a dynamic vibration absorber (DVA), control system, with the incontrovertible truth that it is lightest and more easy to be managed than the mechanical

DVA itself. However, despite its established reputation, the inductive shunt shows some limitations partly due to its passive nature. One let think about the non linear dynamic evolution of structures which cannot be tackle through a control methodology characterized by fixed features [3], [4].

Due to its versatility, an innovative semi-active shunt architecture has been proposed: the switched shunt. Since this control technique is not supposed to be tuned to a specific mechanical mode, it shows more adaptability and stability than the previous one. Moreover, being not necessary any controller, the absence of an external power supply reduces vulnerability to power failure, and makes the switched shunt a self-powered architecture [4].

In the following, a simulation of a vibration control system based on the combined action of inductive-switched shunt circuits is illustrated. As test specimen, a aluminium plate, clamped on the edges, controlled by 9 piezo patches. The possibility of jointly implementing such architectures may guarantee a more efficient multi mode control.

More in detail, after the description of the working principle of the technique, the FE based on simulation strategy is described; finally, achieved simulation results in terms of system mechanical displacements, in time domain are illustrated.

## 2. WORKING PRINCIPLE

To better understand the control strategy of the proposed architecture the working principle of the single inductive and switched shunt technique will be illustrated in this section.

The inductive shunt, is a RLC electric circuit in which the capacitor is substituted by the pzt element. As told in the introduction, this kind of control can be interpreted as a dynamic vibration absorber [5], that is to say a classical mass-spring-damper system. The DVA must be designed in such a way that the system natural frequencies should be as much as possible far off from the exciting frequency.

For sake of simplicity what follows is a sdof mechanical system subjected to an harmonic excitation (see Fig.1):

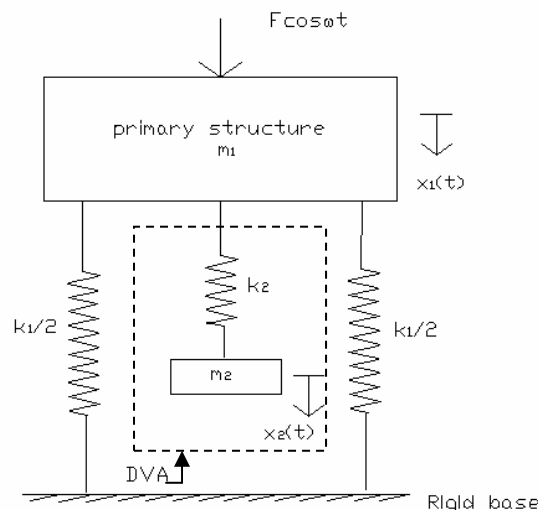


Figure 1. A SDOF mechanical system with a DVA control architecture.

with  $\omega = \sqrt{k_1/m_1}$ . Suppose to connect a second mass  $m_2$  by a spring  $k_2$ , the equations of

motion are:

$$\begin{Bmatrix} m_1 & 0 \\ 0 & m_2 \end{Bmatrix} \begin{Bmatrix} \ddot{x}_1 \\ \ddot{x}_2 \end{Bmatrix} + \begin{Bmatrix} k_1 + k_2 & -k_2 \\ -k_2 & k_2 \end{Bmatrix} \begin{Bmatrix} \dot{x}_1 \\ \dot{x}_2 \end{Bmatrix} = \begin{Bmatrix} F \cos \omega t \\ 0 \end{Bmatrix} \quad (1)$$

with a solution of the form  $x_j = X_j \cos \omega t$  with  $j=1,2$  the complex amplitudes are:

$$X_1(\omega) = \frac{(-m_2\omega^2 + k_2)F}{(-m_1\omega^2 + k_1 + k_2)(-m_2\omega^2 + k_2) - k_2^2} \quad X_2(\omega) = \frac{k_2 F}{(-m_1\omega^2 + k_1 + k_2)(-m_2\omega^2 + k_2) - k_2^2} \quad (2)$$

If  $\omega_{10} = \sqrt{\frac{k_1}{m_1}}$   $\omega_{20} = \sqrt{\frac{k_2}{m_2}}$  the expressions (2) become:

$$X_1(\omega) = \frac{\left(1 - \frac{\omega^2}{\omega_{20}^2}\right) \frac{F}{k_1}}{\left(1 + \frac{k_2}{k_1} - \frac{\omega^2}{\omega_{10}^2}\right) \left(1 - \frac{\omega^2}{\omega_{10}^2}\right) - \frac{k_2}{k_1}} \quad X_2(\omega) = \frac{\frac{F}{k_2}}{\left(1 + \frac{k_2}{k_1} - \frac{\omega^2}{\omega_{10}^2}\right) \left(1 - \frac{\omega^2}{\omega_{10}^2}\right) - \frac{k_2}{k_1}} \quad (3)$$

when  $\omega_{10} = \omega_{20} = \omega$  it results:

$$X_1(\omega) = 0 \quad X_2(\omega) = -\frac{F}{k_2} \quad (4)$$

In other words, when tuned on the resonance frequency, the primary structure does not vibrate because the mass  $m_2$  transmits to the  $m_1$  a force equal and opposite respect to the external excitation signal. If the mass-spring-damper system is now substituted by an inductive-capacitive-resistive circuit, with the pzt element as capacitor, that is to say an “inductive shunt” circuit (see Fig.2.A), the control system is able to reduce dump vibrational energy of the structure when opportunely tuned on the primary structure resonance frequency:

$$\omega = \sqrt{\frac{k_1}{m_1}} = \frac{1}{\sqrt{LC_{pzt}}} \quad (5)$$

being  $\omega = \frac{1}{\sqrt{LC_{pzt}}}$  the electric resonance.

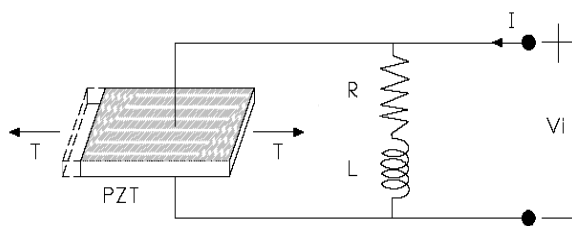


Figure 2.A-An inductive shunt circuit

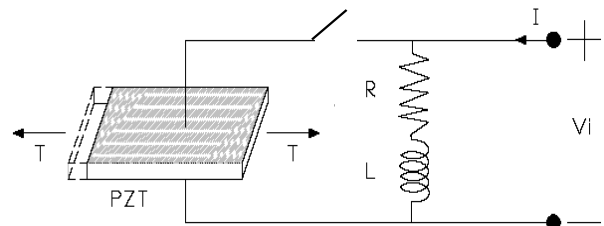


Figure 2.B-A switched shunt circuit

The mechanical vibrations are transduced by the pzt electromechanical constants into voltage. At the resonance, the inductive element allows the voltage reversing on the pzt electrodes inducing a phase lag between pzt action and structure displacement, with consequent damping. Anyway it is clear that if the primary structure dynamics suddenly change, the inductive shunt circuit results detuned, losing the most of its efficiency. Moreover if the frequency to be controlled is low, required inductor would result too high to be feasible. To exceed this limitations the switched shunt architecture has been investigated. This circuit is quite different from the previous one for the introduction of a switch component (Fig.2.B). During the dynamic evolution of the primary structure, the switch device is generally open. Only when the maxima deformation is reached, the switch will be closed for a very short period if compared with the normal mode period to be controlled. During the closed loop state, the circuit architecture looks like an inductive shunt, with the essential difference that the “inductive” performance is now time limited to the shutting time period and that it is not tuned on the frequency to be controlled. This strategy allows to obtain damping through the pzt transmitted actions comparable to a pulse signal (see Fig.4). Since the switched shunt circuit is not supposed to be tuned to mechanical resonances, it results in a more efficient and flexible strategy compared to the resonance circuit without switched shunt concerning e.g. control in the low frequencies range.

For example if the shutting time period is a fraction  $n$  of the mechanical vibration of interest, the frequency  $f_{el}$  will be related to the mechanical one:

$$f_{el} = n f_{mech} \quad \text{with} \quad L = \frac{1}{4\pi^2 f_{el}^2 C_{pzt}} \quad (6)$$

thus, the required inductance will be  $n$  times lower than the one required by an inductive architecture for the same frequency. Moreover, the methodology adopted allows this control system to be quite independent from the dynamic evolution of the structure, resulting as a more adaptable and “fault tolerant” architecture. To achieve this result, the  $RLC_{pzt}$  parameters of the switch circuit can be chosen, for example, so that its electrical frequency is coincident with a higher structural mode to be controlled [4].

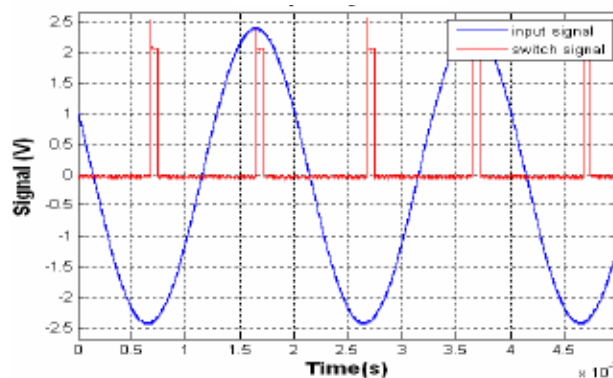


Figure 4. Time evolution of the Switched Shunt characteristic signal: input signal (blue line) and switch signal (red line).

The possibility of jointly implementing both a switched and an inductive shunt architecture may guarantee a more efficient multi mode control. As a matter of fact, it is possible to

simultaneously control a low and a high frequency mode through a combined action of the described techniques.

### 3. SIMULATION STRATEGY

In what follows the simulation strategy to perform the combined switched-inductive control is presented. An anisotropic aluminium plate with clamped edges is taken into account. The control system is constituted by a pzt network bonded on one surface of the primary structure. The integrated electro-mechanic system is described by the following dynamic equation:

$$\begin{bmatrix} \underline{\underline{M}} & 0 \\ 0 & \underline{\underline{L}} \end{bmatrix} \begin{Bmatrix} \ddot{x} \\ \ddot{q} \end{Bmatrix} + \begin{bmatrix} \underline{\underline{B}} & 0 \\ 0 & \underline{\underline{R}} \end{bmatrix} \begin{Bmatrix} \dot{x} \\ \dot{q} \end{Bmatrix} + \begin{bmatrix} \underline{\underline{K}} & \underline{\underline{D}} \\ \underline{\underline{G}} & \underline{\underline{K}}_e \end{bmatrix} \begin{Bmatrix} x \\ q \end{Bmatrix} = \begin{Bmatrix} F \\ 0 \end{Bmatrix} \quad (7)$$

being  $M$ ,  $B$  and  $K$  the mass, damping and the stiffness matrices for the primary structure, extracted through the FE model of the plate (see Par.4) in Nastran environment;  $L$ ,  $R$ ,  $K_e$ , the inductive, resistive and pzt-capacitive matrices of the control system;  $D$  and  $G$  the electromechanical coupling pzt matrices [5], [6],  $F$  the external force and  $x$  and  $q$  respectively the structural and electric dofs, that is to say the pzt charge. In the case of a pzt network the electric matrices will specialised in the following manner:

$$\underline{\underline{L}} = \begin{bmatrix} L_{p_1} & 0 & 0 & \cdot & \cdot & \cdot & \cdot & 0 \\ 0 & L_{p_2} & 0 & \cdot & \cdot & \cdot & \cdot & 0 \\ 0 & 0 & L_{p_3} & \cdot & \cdot & \cdot & \cdot & 0 \\ \cdot & \cdot \\ \cdot & \cdot & \cdot & \cdot & L_{p_i} & \cdot & \cdot & \cdot \\ \cdot & \cdot \\ \cdot & \cdot & \cdot & \cdot & \cdot & \cdot & L_{p_{p_c-1}} & 0 \\ 0 & 0 & 0 & \cdot & \cdot & \cdot & 0 & L_{p_{p_c}} \end{bmatrix} \quad \underline{\underline{R}} = \begin{bmatrix} R_{p_1} & 0 & 0 & \cdot & \cdot & \cdot & \cdot & 0 \\ 0 & R_{p_2} & 0 & \cdot & \cdot & \cdot & \cdot & 0 \\ 0 & 0 & R_{p_3} & \cdot & \cdot & \cdot & \cdot & 0 \\ \cdot & \cdot \\ \cdot & \cdot & \cdot & \cdot & R_{p_i} & \cdot & \cdot & \cdot \\ \cdot & \cdot \\ \cdot & \cdot & \cdot & \cdot & \cdot & \cdot & R_{p_{p_c-1}} & 0 \\ 0 & 0 & 0 & \cdot & \cdot & \cdot & 0 & R_{p_{p_c}} \end{bmatrix} \quad (8)$$

with

$$\forall i \in [1,9] \quad L_i = \begin{cases} \frac{1}{\omega^2 C_{pzt}} \\ \frac{1}{n\omega^2 C_{pzt}} \end{cases} \quad R_i = \begin{cases} R_{opt} \\ R \rightarrow \infty \\ R \rightarrow 0 \end{cases} \quad (9)$$

The first position relating the  $L$  value to the inductive shunt configuration while the second to the switched one. At the same manner the resistive matrix with the first position relating the  $R$  value to the inductive shunt configuration while the second to the switched one, according respectively to the open and closed loop state of the circuit.

The idea is to control two structural modes, simultaneously, by adopting the same piezos and the same circuit. To this aim:

- The switch architecture has to be used to control a low frequency mode.
- The inductive architecture has to be used to control an higher frequency mode, being the required inductance suitably lower for high frequencies.

Thus the conditions to be satisfied for the inductive and switch architectures will be the sequent:

$$\forall i \in [1..9] \quad \omega_i = \frac{1}{\sqrt{L_i C_{pzt_i}}} = \omega_{m,high} \quad \text{and} \quad \omega_i = \frac{1}{\sqrt{L_i C_{pzt_i}}} \geq n \cdot \omega_{m,low} \quad (10)$$

inductive shunt
switched shunt

with

$$n = \frac{\omega_{m,high}}{\omega_{m,low}} \quad (11)$$

#### 4. THE NUMERIC MODEL

According to the preceding data, the model validation campaign is performed through a preliminary numerical simulation [6]. In Femap environment the finite element model of the aluminum plate with the PZT net is realized (see Fig.5).

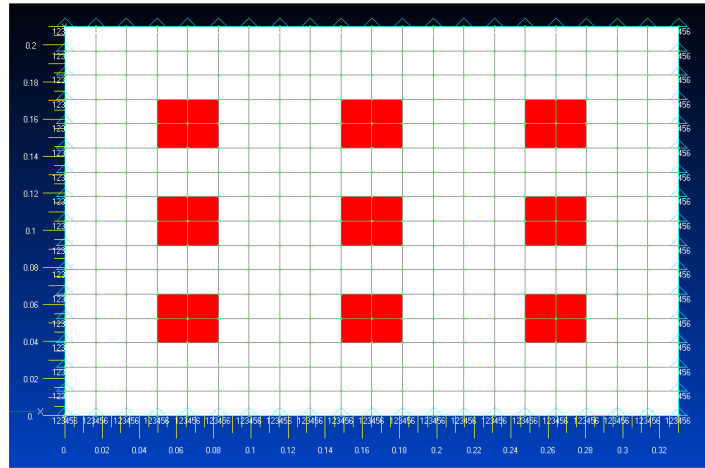


Figure 5. Plate FE Model and pzt spatial configuration

Table 1. FE Model main features.

Parameter	Value
Element type	CQUAD
Constrained condition	Fixed
Node number	357
Structure Material	Al 7075 T6
Young's modulus, $E$ (GPa)	72.0
Density, $\rho$ ( $\text{kg/m}^3$ )	2750
Poisson's ratio, $\nu$	0.32
Thickness, $h$ (mm)	1.0
In-plane dimensions (m)	0.33 x 0.21

Table 2. Piezo features.

Parameter	Value
In-plane dimensions (mm)	33 x 26
Thickness, $t_p$ (mm)	0.5
Poisson's ratio, $\nu$	0.32
Young's modulus, $E$ (GPa)	59.0
$d_{31}$ (C/N)	350.e-12
$\epsilon_r$	5000

## 5. RESULTS

Finally, the structural output is computed using a set of coupled equations through direct numerical integration. An optimized integrator solver (based on the Newmark-Beta solving technique) has been implemented to compute system response.

Due to the no stationary nature of the adopted technique, time responses of the structure, with and without control, have been estimated (see Fig.6,7,8 (A,B)):

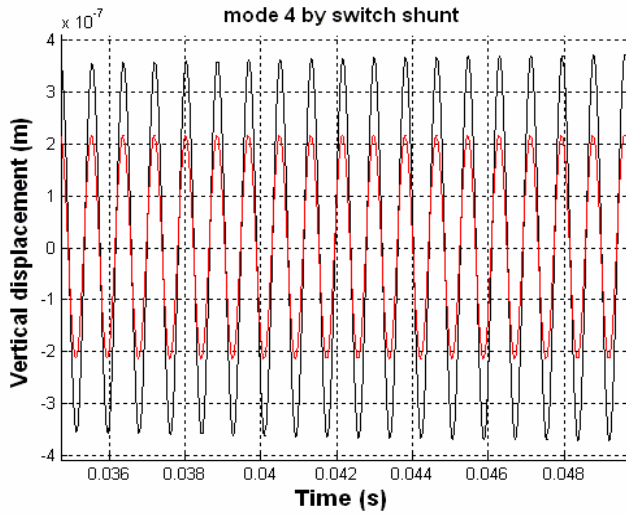


Figure 6.A. Mode 4 by switch shunt control

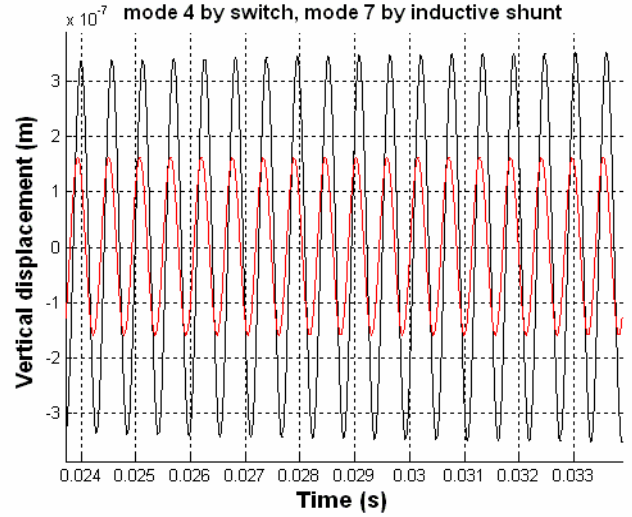


Figure 6.B. Mode 4 by switch and mode 7 by inductive control

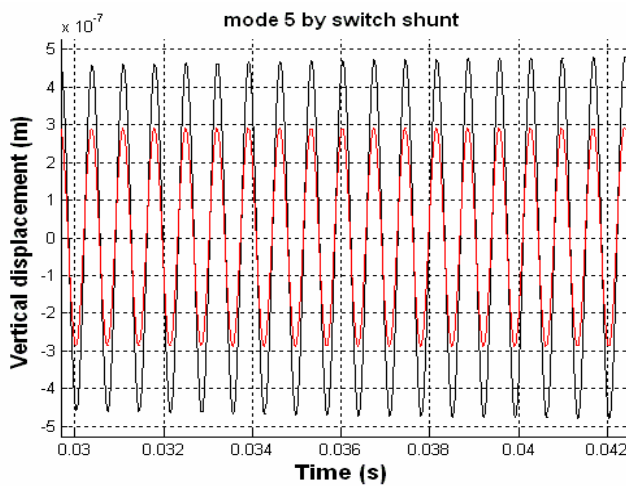


Figure 7.A. Mode 5 by switch shunt control

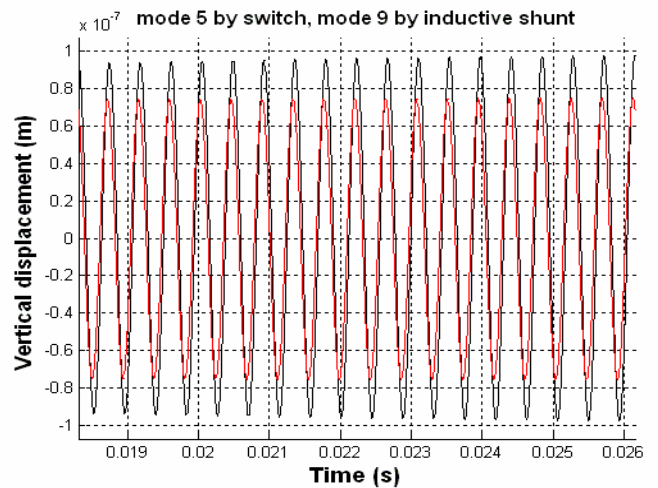


Figure 7.B. Mode 5 by switch and mode 9 by inductive control

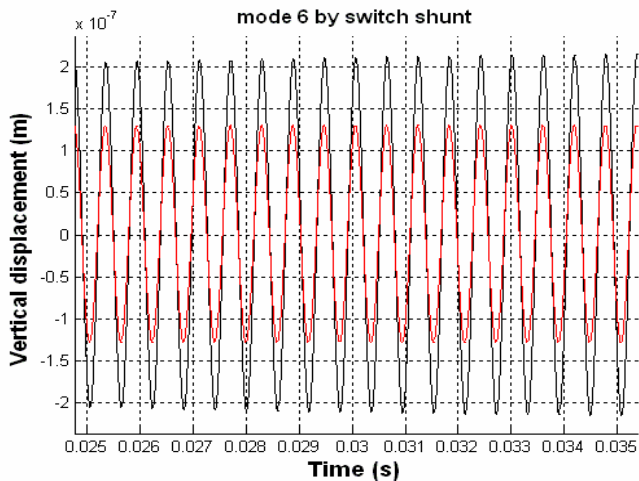


Figure 8.A. Mode 6 by switch shunt control

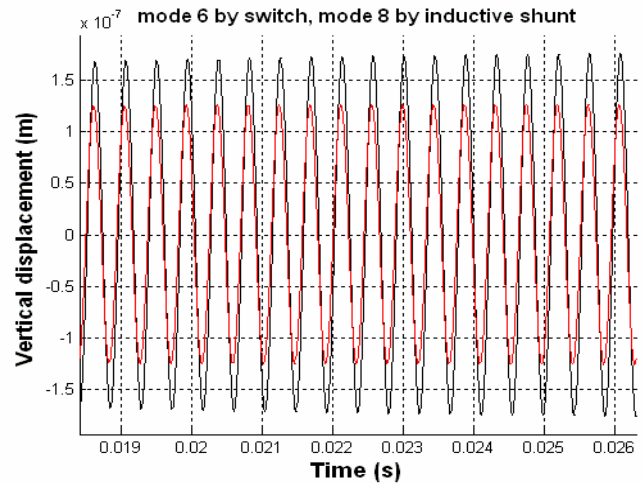


Figure 8.B. Mode 6 by switch and mode 8 by inductive control

## 6. CONCLUSIONS

In this paper, the possibility of controlling vibrations by implementing simultaneously a switched and an inductive architecture has been considered. More in detail, one has taken advantage of the ability of the switched and inductive shunt architectures of controlling low and high frequencies, respectively. As a matter of fact, being not required any tune operation for the switch control, it is possible to choose the inductance of the circuit so that it could assure a short switching and, at the same time an electric frequency coincident with the larger structural one. Numerical results have been obtained by coupling one of the first 6 modes of the structural system, with the next ones (7-12), by obtaining a max reduction of the 50% of the amplitude. The best results in terms of amplitude attenuation have been presented in this work.

## REFERENCES

- [1] L.R. Corr., W.W. Clark,: "Comparison of Low Frequency Piezoceramic Shunt Techniques for Structural Damping." *SPIE Proceedings*, Vol. 4331, 262-272 (2001)
- [2] C. Richard,, D. Guyomar,, D. Audigier, H. Bassaler,: "Enhanced Semi-Passive Damping using Continuous Switching of a Piezoelectric Device on an Inductor" *SPIE Proceedings*, Vol. 3989, 288-299
- [3] M. Ciminello, S. Ameduri, A. Concilio, "Semiactive Vibration Control using Piezoelectrics in Shunt Configuration", The Italian Aerospace Research Center, CIRA scpa –*The Second International Conference on Dynamics, Vibration and Control (ICDVC 2006) Beijing, China*, August 23-26, 2006 - No.ICDVC2006-w72.
- [4] M. Ciminello, S. Ameduri, A. Calabrò, A. Concilio "Synchronised Switched Shunt Control Technique Applied on a Cantilevered Beam: Numerical and Experimental Investigations", The Smart Structures Laboratory - The Italian Aerospace Research Center, CIRA. *Submitted to JIMSS, assigned number JIMSS-06-100.*
- [5] M. Ciminello, S. Ameduri, A. Concilio "FE Modelling of an Innovative Vibration Control Shunt Technique", , The Smart Structures Laboratory – The Italian Aerospace Research Center, CIRA. *Submitted to JIMSS, assigned number JIMSS-06-074.*
- [6] M. Ciminello, S. Ameduri, A. Concilio "Numerical Simulation of a Switched Shunt based on Network, acting on a Glass Fibre Panel", The Italian Aerospace Research Center, CIRA scpa –*The Fifth Asian-Australian Conference on Composite Materials (ACCM-5) Hong Kong*, November 27-30, 2006.